Influence of Ultrasonic Frequency on Swan Band Sonoluminescence and Sonochemical Activity in Aqueous Tert-Butanol Solutions.

ARTICLE *in* THE JOURNAL OF PHYSICAL CHEMISTRY B · DECEMBER 2014

Impact Factor: 3.3 · DOI: 10.1021/jp509898p · Source: PubMed

4 AUTHORS:

Rachel Pflieger
Institut de Chimie Séparative de Marcoule
32 PUBLICATIONS **188** CITATIONS
SEE PROFILE

Abdoul Aziz Ndiaye
Université du Maine
7 PUBLICATIONS **35** CITATIONS
SEE PROFILE

Tony Chave
Institut de Chimie Séparative de Marcoule
31 PUBLICATIONS **393** CITATIONS
SEE PROFILE

Sergey Nikitenko
Atomic Energy and Alternative Energies Com…
79 PUBLICATIONS **1,223** CITATIONS
SEE PROFILE

THE JOURNAL OF PHYSICAL CHEMISTRY B

Article

pubs.acs.org/JPCB

Influence of Ultrasonic Frequency on Swan Band Sonoluminescence and Sonochemical Activity in Aqueous *tert*-Butyl Alcohol Solutions

Rachel Pflieger, Abdoul Aziz Ndiaye, Tony Chave, and Sergey I. Nikitenko*

Institut de Chimie Séparative de Marcoule, UMR5257, CEA-CNRS-UM2-ENSCM, Centre de Marcoule, Bat. 426, BP 17171, 30207 Bagnols-sur-Cèze, France

Supporting Information

ABSTRACT: The multibubble sonoluminescence (MBSL) spectra of *t*-BuOH aqueous solutions submitted to power ultrasound at 20, 204, 362, and 613 kHz show emissions for the $\Delta v = -1$ to $\Delta v = +2$ vibrational sequences of C_2* Swan system ($d^3\Pi_g \rightarrow a^3\Pi_u$). The Δv=+2 emission overlaps with the CH(A−X) emission band. The maximal Swan band emission is observed when the MBSL of water itself is almost completely quenched. In general, MBSL is more intense at high-frequency compared to 20 kHz ultrasound. However, in the presence of Xe, the MBSL of C_2* at 20 kHz is so bright that it can be seen by the unaided eye as a blue glow in the close vicinity of the ultrasonic tip. The intensity of the C_2* band emission exhibits a maximum vs *t*-BuOH concentration: 0.1−0.2 M at 20 kHz and (1−8) × 10^{-3} M at high-frequency ultrasound. Such a huge difference is attributed to a much smaller bubble size at high ultrasonic frequency or, in other words, to a much higher bubble surface/volume ratio providing more efficient saturation of the bubble interior with *t*-BuOH vapors and to the fact that high frequency bubbles remain active for many more cycles than 20 kHz ones, thus accumulating more hydrocarbon decomposition products. Simulation of the emission spectra using Specair software demonstrated the absence of thermal equilibrium for C_2* radicals ($T_v > T_r$), where T_v and T_r are the vibrational and the rotational temperature, respectively. In Ar, T_v decreases with increasing *t*-BuOH concentration reaching a steady value in the concentration domain that corresponds to C_2* emission maximum intensity. In the presence of Xe an extremely high T_v is obtained, which is explained by the relatively low ionization potential of Xe providing a higher electron temperature of nonequilibrium plasma generated during bubble collapse. Analysis of the gaseous products of *t*-BuOH sonolysis reveals a significant sonochemical activity even at high *t*-BuOH concentration when MBSL is totally quenched, indicating that drastic conditions could be produced also within nonsonoluminescing cavitation bubbles.

1. INTRODUCTION

Multibubble sonoluminescence (MBSL) spectra from organic solvents[1,2] or from aqueous solutions of organic compounds[3,4] often show emission from excited C_2* radicals. The most intense emission lines of these species, known as the Swan band system ($d^3\Pi_g \rightarrow a^3\Pi_u$), are easily detectable in flames or plasmas containing carbon for the $\Delta v = -3$ to $\Delta v = +2$ sequences in the visible spectral range.[5] The relative populations of Δv levels are sensitive to C_2 vibrational temperature (T_v).[5,6] Therefore, Swan band emission is traditionally employed as a molecular probe to evaluate the temperatures of flames and plasmas. Similar measurements of C_2* MBSL in water/benzene mixture and silicone oil submitted to low-frequency 20 kHz ultrasound provided an intrabubble gas temperature (T_g) in the range of 4000−5000 K presuming thermal equilibrium inside the collapsing bubble ($T_v \approx T_g$).[2,3] However, recent spectroscopic studies of $OH^\bullet$ radicals MBSL in water saturated with Ar or Xe revealed the formation of a nonequilibrium plasma during multibubble cavitation.[7] The vibrational excitation of $OH(A^2\sum^+)$ state was shown to be much stronger at high ultrasonic frequency compared to 20 kHz ultrasound. In contrast to $OH^\bullet$ radicals that arise from the sonolysis of water molecules, C_2* excited species are formed as products of a complex set of chemical reactions occurring inside the cavitation bubbles. Therefore, MBSL of C_2* can be useful to study the mechanism of organic compounds sonolysis in addition to its application for cavitation thermometry. However, the relationship between sonochemical activity and sonoluminescence spectroscopy has just begun to emerge. To the best of our knowledge, the MBSL of Swan band has never been reported at high-frequency ultrasound (≥100 kHz). This paper focuses on the effect of ultrasonic frequency on Swan band emission spectra in aqueous solutions of *tert*-butyl alcohol (*t*-BuOH). Another aim of the study is to find out the correlation between MBSL spectra and sonochemistry of *t*-BuOH in aqueous solutions.

2. EXPERIMENTAL METHODS

2.1. Materials. *tert*-Butyl alcohol (≥99.5%) and other analytical grade chemicals were purchased from Aldrich and

Received: September 30, 2014
Revised: December 10, 2014
Published: December 12, 2014

DOI: 10.1021/jp509898p
J. Phys. Chem. B 2015, 119, 284−290

used without further purification. Deionized water (Milli-Q 18.2 MΩ cm) was used to prepare all solutions. Argon and xenon at 99.999% purity were provided by Air Liquide.

2.2. Reactor Setup and Analytical Procedures. The experiments have been performed at 20, 204, 362, and 613 kHz using the multifrequency sonoreactor described recently.[7] The absorbed acoustic power measured by thermal probe method was found to be equal to 25 W at 20 kHz, 32 W at 204 kHz, and 43 W at 362 and 613 kHz. For all experiments, 250 mL of the solutions were sparged with inert gas about 30 min before sonication and during the ultrasonic treatment at a controlled rate of 100 mL min^{-1}. The temperature of the sonicated solutions was maintained with a Huber Unistat Tango cryostat, at 11 °C for 20 kHz, and at approximately 5 °C for high-frequency ultrasound.

The MBSL spectra were collected in the spectral range 240−600 nm using a SP 2356i Roper Scientific spectrometer (gratings 300blz300 and 150blz500, slit width 0.25 mm) coupled to a liquid-nitrogen-cooled CCD camera (SPEC10−100BR Roper Scientific). For each experiment, at least three 300-s spectra were averaged and corrected for the background noise and for the quantum efficiencies of gratings and CCD. The MBSL spectra generated by 20 kHz ultrasound were collected in the vicinity of the ultrasonic tip, where the highest light emission intensity was provided.

Gaseous products of sonolysis at 20 kHz and 362 kHz were measured using a quadrupole mass spectrometer (PROLAB 300, Thermo Fisher). The multiple ion monitoring (MIM) mode was employed to follow the evolution of H_2, C_2H_2, CH_4, CO, and CO_2 during sonolysis. The rates of gaseous products formation were determined after mass spectrometric data calibration with corresponding gas mixtures provided by Messer. The accuracy for the reaction rates measurements was estimated to be 10−20%. Water vapor in the outlet gas was trapped with molecular sieves (Aldrich, 3 Å) prior to the mass spectrometric analysis.

3. RESULTS AND DISCUSSION

3.1. Intensity of MBSL. The MBSL spectra in argon-saturated water exhibit the emission of $OH^•$ radicals from $OH(A^2\Sigma^+)$ and $OH(C^2\Sigma^+)$ excited states as well as a broad continuum ranging from UV to near-infrared range (Figure 1) in agreement with recently published data.[7] The addition of *t*-BuOH causes a sharp decrease of the overall MBSL intensity. On the other hand, the MBSL spectra in the presence of *t*-BuOH show emissions for the $\Delta\nu = -1$ to $\Delta\nu = +2$ vibrational sequences of C_2* Swan system (Figure 1). Note that the acoustic power at 20 kHz (25 W) was lower than that at 359 kHz (43 W). Such difference could impact the total intensity of MBSL since the number of cavitation bubbles will be changed with ultrasonic power. However, the preliminary experiments revealed that the power in the presently studied range has only a limited influence on the relative peak intensities of OH(A−X) and C_2 systems.

Figure 2 demonstrates that in contrast to the strong decrease in overall intensity of sonoluminescence with *t*-BuOH concentration the relative intensity of C_2* emission exhibits a maximum at some optimal *t*-BuOH concentrations. The striking feature is the huge difference in these concentrations between low- and high-frequency ultrasound. Table 1 reveals that the strongest C_2* emission lines are observed at 0.1−0.3 M and 0.9×10^{-3} to 7.5×10^{-3} M of *t*-BuOH for 20 kHz and 204−613 kHz, respectively. In other words, a much higher

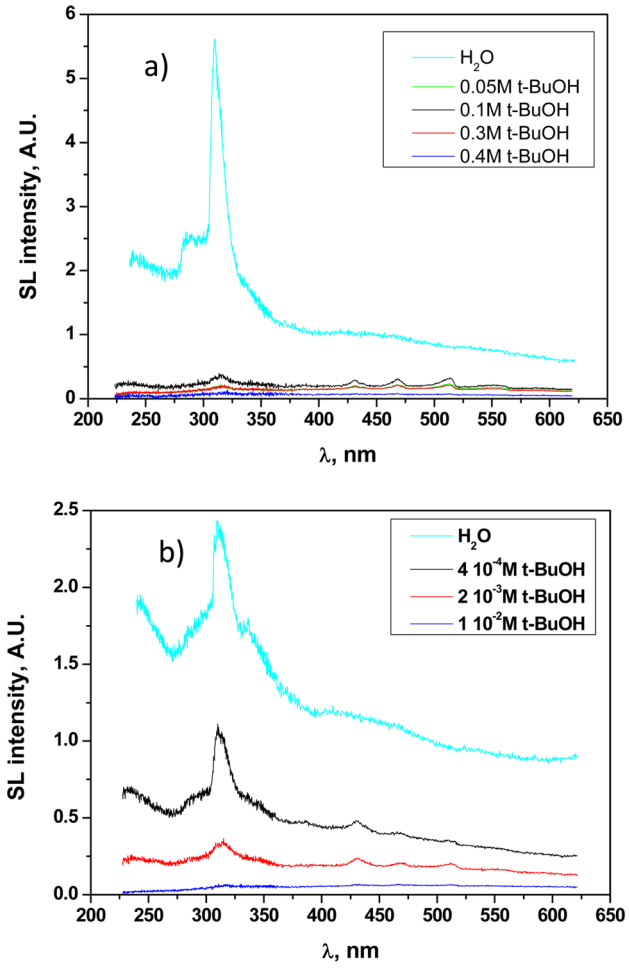

Figure 1. MBSL spectra in water and *t*-BuOH solutions at 20 kHz (a) and 204 kHz (b) in the presence of argon: (a) P = 25 W, 11 °C; (b) LP = 54 W, P_{ac} = 32 W, 4−8 °C.

concentration of *t*-BuOH is required to provide maximal C_2* MBSL at 20 kHz compared to high-frequency ultrasound. On the other hand, in the studied range of high ultrasonic frequencies the optimal range of *t*-BuOH concentrations is approximately independent from the frequency.

As evidenced in Figure 2 the maximal Swan band emission is observed when the overall MBSL is almost completely quenched. The decrease of MBSL under continuous sonication of water in the presence of volatile organics has been already reported by several authors[3,8] and attributed to endothermic chemical reactions that would consume some of the energy, thus lowering the intrabubble temperature. Alternatively, this may also be due to nonradiative scavenging of excited species originating from water sonolysis ($OH^•$, H_2O*) by the molecules of organic compounds incorporated within the cavitation bubbles leading to C_2* intermediate formation and to a decrease of radiative recombination by consumption of H and OH radicals through reactions with the organic species. Both phenomena have been observed in flames and plasmas.[3,9] Consequently, the accumulation inside the bubble of *t*-BuOH vapor and of hydrocarbon products issued from *t*-BuOH degradation will quench MBSL of water and enhance C_2* emission. In this view, the significant difference in $[t\text{-BuOH}]_{max}$ values for low- and high-frequency ultrasound could be related to the decrease in bubble size with ultrasonic frequency. As the bubble size decreases, its surface-to-volume ratio rises ($S/V \sim$

DOI: 10.1021/jp509898p
J. Phys. Chem. B 2015, 119, 284−290

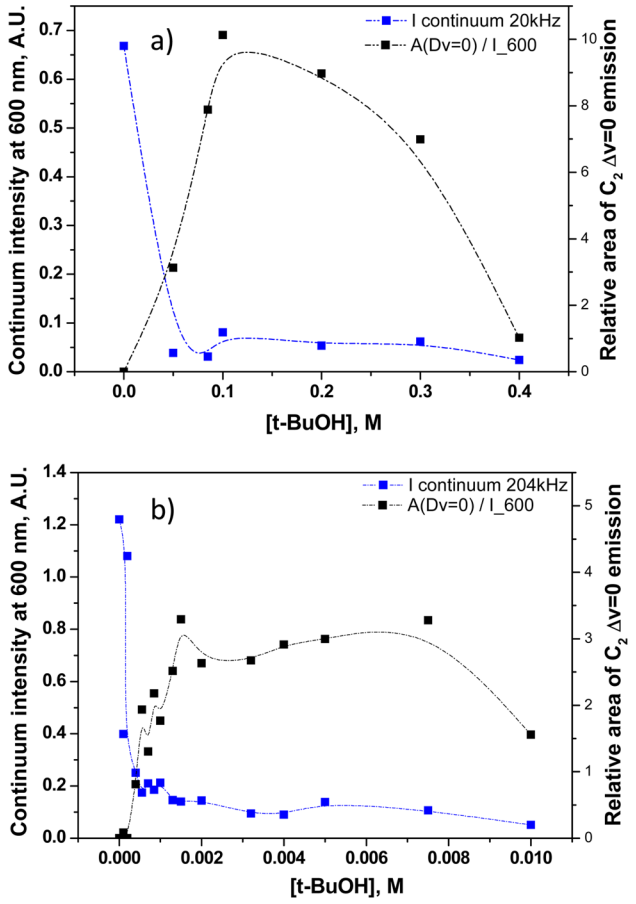

Figure 2. Influence of *t*-BuOH concentration on MBSL emission intensity measured at 600 nm (continuum emission) and on the relative intensity of C_2* ($\Delta\nu = 0$) emission, for 20 kHz (a) and 204 kHz (b). Dash-dotted lines are only there for clarity.

Table 1. Optimal Range of *t*-BuOH Concentrations, $[t\text{-BuOH}]_{max}$, for the Observation of Maximal Swan Band Emission Intensity, as a Function of Ultrasonic Frequency

frequency, kHz	$[t\text{-BuOH}]_{max}$, M
20	0.09−0.3
204	0.9×10^{-3} to 7.5×10^{-3}
362	1.0×10^{-3} to 5.0×10^{-3}
613	1.0×10^{-3} to 5.0×10^{-3}

$1/r$), which provides a more effective saturation of the bubble interior with volatile solutes through evaporation at the bubble wall. Computer simulations[10] calculated ambient radii of 0.1−100 μm at 20 kHz and of 0.1−10 μm at 140 kHz, thus much larger bubbles at low frequency. Besides, it has been suggested that 20 kHz bubbles would show a transient behavior while high frequency ones would undergo more oscillations before collapsing.[8b] This higher number of oscillations allows more *t*-BuOH evaporation into the bubbles but also accumulation at each oscillation of hydrocarbon decomposition products and hence higher SL quenching at the same concentration of the solution. On the other hand, both the bubble dynamics and the bubble size are very similar between high frequencies (e.g., experimental measurements[11] revealed that in the frequency range of 200−650 kHz the ambient bubble radii are characterized by broad, partly overlapping distribution functions centered in the presence of air at 3.9, 3.2, and 2.9 μm for 213, 355, and 647 kHz respectively), which can explain the insignificant effect of the studied high ultrasonic frequency on the optimal *t*-BuOH concentrations. Note that the bulk temperature was 11 °C at 20 kHz and 5 °C at 359 kHz. At lower bulk temperature, *t*-BuOH vapor pressure is lower and it will evaporate less into bubbles. Thus, a higher concentration of *t*-BuOH in solution would be needed to get the same amount of *t*-BuOH in bubbles. This means the concentration range for which C_2 emission is maximal at 20 kHz would probably be a little bit shifted to higher concentrations at a bulk temperature of 5 °C, thus even further from the concentration range at high frequency. For a difference of 6 °C, the vapor pressure change is about 30%, which is negligible compared to the 2 orders of magnitude between the low and high frequency concentration ranges.

3.2. Rovibronic Temperatures of C_2* Radicals. Figure 3 reveals that the ultrasonic frequency strongly affects not only the overall intensity of MBSL but also the shape of the Swan band emission spectrum. In argon, the relative intensity of the $\Delta\nu = +1$ branch is higher at 362 kHz than at 20 kHz. Interesting is that replacing argon with xenon leads to a significant increase of the $\Delta\nu = +1/\Delta\nu = 0$ ratio even at low-frequency ultrasound (Figure 3c). Moreover, at 20 kHz in the presence of xenon, the Swan band MBSL is so bright that it can be seen by the unaided eye as a blue conical glow near the horn tip (Figure 3d). Note here that the light emission from water itself ($OH^{\bullet}$ radicals and continuum) is strongly reduced at these conditions.

The most intense $\Delta\nu = 0$, $\Delta\nu = +1$, and $\Delta\nu = +2$ branches of the Swan band system are composed of (0−0), (1−1), (2−2), (3−3), (4−4); (1−0), (2−1), (3−2), (4−3), (5−4), (6−5), and (2−0), (3−1), (4−2), (5−3), (8−6) vibration−vibration transitions, respectively.[12] The $\Delta\nu = +2$ branch overlaps with $A^2\Delta - X^2\Pi(\Delta\nu = 0)$ emission band of CH* radical which is often formed during high-temperature pyrolysis of organic molecules or via the oxidation of C_2* by $OH^{\bullet}$ radicals.[13] One can see that the higher vibrational states of C_2* contribute to $\Delta\nu = +1$ branch in higher extent than to $\Delta\nu = 0$ branch. Therefore, the relative increase of $\Delta\nu = +1$ band intensity indicates higher vibrational excitation of C_2* radical, as is also evidenced in simulations of plasma emission spectra.[14]

Vibrational (T_v) and rotational (T_r) temperatures of C_2* radicals were calculated from $\Delta\nu = 0$ and $\Delta\nu = +1$ lines of Swan band system using Specair software widely applied in physics of low-temperature plasma.[14] Obtained temperatures as a function of *t*-BuOH concentration are exemplified in Figure 4 for 204 kHz ultrasound. Other examples of emission spectra, their fits and the evolution of rovibronic temperatures with *t*-BuOH concentration are shown in Supporting Information. At very low *t*-BuOH concentrations, in the range where the overall SL intensity is strongly decreased and the intensity of C_2* emission increases (see Figure 2), C_2* vibrational temperature is seen to decrease. It then reaches a steady value in the concentration domain that corresponds to C_2* emission maximum intensity. Vibrational and rotational temperature values on this plateau are summarized in Table 2. Taking into account the strong coupling between translational and rotational energy states, the rotational temperature is in the general case close to the gas temperature ($T_r \sim T_g$). The here-determined rovibronic temperatures clearly indicate the absence of thermal equilibrium for C_2* radicals ($T_v > T_g$), which is in agreement with the formation of a nonequilibrium plasma inside the collapsing bubbles as recently reported.[7] Moreover, there is a striking

DOI: 10.1021/jp509898p
J. Phys. Chem. B 2015, 119, 284−290

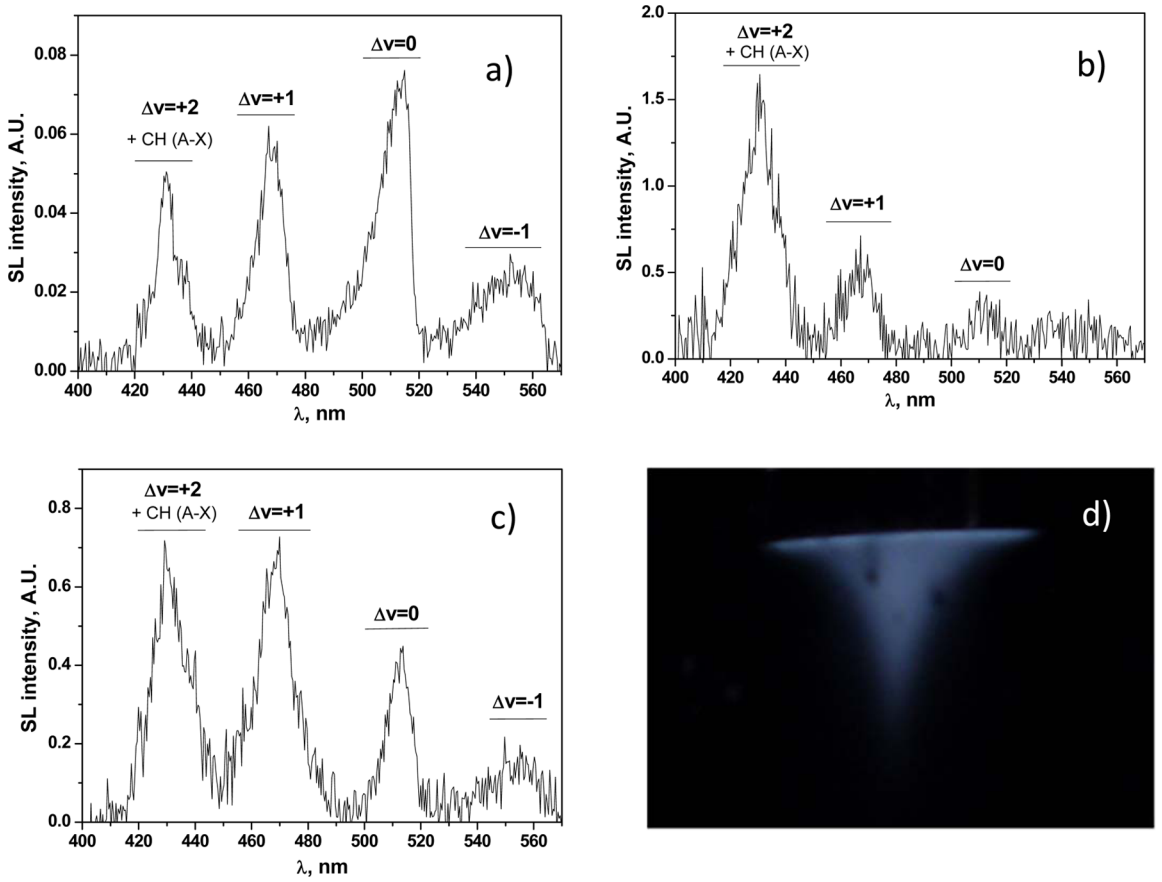

Figure 3. Swan band MBSL spectra with subtracted baselines measured at optimal *t*-BuOH concentration. (a) 20 kHz, Ar, 0.1 M *t*-BuOH, 11 °C, (b) 362 kHz, Ar, 8.5 × 10^{-4} M *t*-BuOH, 5 °C, (c) 20 kHz, Xe, 0.1 M *t*-BuOH, 11 °C, (d) photograph of C_2* MBSL at 20 kHz, Xe, 0.1 M *t*-BuOH, 11 °C, exposure time = 30 s. The picture is taken through the quartz window of the sonoreactor.

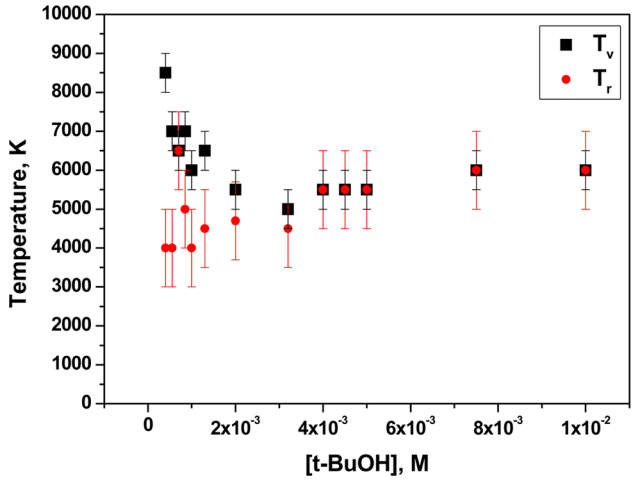

Figure 4. Influence of *t*-BuOH concentration on C_2 vibrational and rotational temperatures, 204 kHz, P_{ac}= 32W, 6 °C. The uncertainties have been obtained from the optimized fits performed by Specair software. Similar plots for other frequencies and fits of the experimental spectra are shown in Supporting Information.

similarity in the behavior of C_2* radicals studied in this work and that of OH• radicals reported for sonicated water,[7a,b] with replacing argon with xenon leading to a sharp increase in T_v. On the other hand, the T_v values of C_2* at very low *t*-BuOH concentration were found to be higher than those of OH• whatever the frequency (Figure 4 and data in Supporting Information). This could be attributed to the systematic underestimation of OH• vibrational temperature related to the calculation code recently developed.[7a] Indeed, OH($A^2\Sigma^+$) T_v were determined based on v = 1 and v = 2 relative populations using a simple Boltzmann model. As a matter of fact, the vibrational populations of OH($A^2\Sigma^+$) state exhibit a Treanor behavior with vibrational overexcitation. Therefore, the real T_v values of OH• should be somewhat higher than those given in Table 2. At higher *t*-BuOH concentrations and high frequency, however, T_v values found for C_2 are lower than previously determined OH T_v values. This may be attributed to the

Table 2. Calculated T_v and T_r Temperatures of C_2 Radicals as a Function of Experimental Conditions in Comparison with Published Data for OH• Radicals[a]

			C_2*		OH($A^2\Sigma^+$)
frequency, kHz	gas	[t-BuOH], M	T_v, K	T_r, K	T_v, K
20	Ar	0.05−0.3	6300	4800	5000 (H_2O)[7b]
20	Xe	0.12	14000	2500	7900 (H_2O)[7a]
204	Ar	4 × 10^{-3} to 1 × 10^{-2}	5800	5800	7600 (H_2O)[7b]
362	Ar	3.2 × 10^{-3} to 7.5 × 10^{-3}	8000	4000	8500 (H_2O)[7b]
613	Ar	2 × 10^{-3} to 5 × 10^{-3}	5000	4000	9000 (H_2O)[7b]

[a]The uncertainty was estimated to be 500 K for T_v and 1000 K for T_r taking into account that T_r values are estimated from the bandwidth of $\Delta\nu$ = +1 and $\Delta\nu$ = 0 branches.

DOI: 10.1021/jp509898p
J. Phys. Chem. B 2015, 119, 284−290

quenching of vibrationally exited C_2 radicals in the presence of large amounts of *tert*-butyl alcohol and the products of its sonolysis.

Using a similar thermometric approach of Swan band emission, Didenko et al.[3] estimated T_v from C_2 emission in Ar-saturated water containing benzene sonicated with 20 kHz ultrasound. They obtained a temperature of 4300 ± 200 K, thus quite lower than the presently determined 6300 ± 500 K. This difference can be explained by the difference in molecular precursor of C_2: benzene has a higher vapor pressure (10 kPa at 20 °C, vs 4.1 kPa for *t*-BuOH) and a higher hydrophobicity, which means that it will evaporate more into expanding cavitation bubbles and also produce more hydrocarbon decomposition products. This statement is in agreement with the difference between both works in the concentration ranges leading to maximum C_2 emission: $1-4.5 \times 10^{-3}$ M for benzene[3] vs 0.1−0.2 M for *t*-BuOH at 20 kHz. Besides that, the C_2 vibrational temperature might reflect the consequence of the chemical reactions leading to C_2 formation in addition to intrabubble conditions. The more intense CH emission in *t*-BuOH solutions (Figure 3) compared to benzene[3] clearly indicates the difference in the mechanisms of sonolysis for these species, which could lead to different rovibronic temperatures of the intermediates.

Okitsu et al.[15] and Ciawi et al.[16] also determined bubble temperatures in aqueous *tert*-butyl alcohol solutions, and obtained values below 4500 K whatever the ultrasonic frequency. However, the chemical thermometry used in these studies yields an average temperature of the bubble, both in time and volume, while SL measurements focus on the spectroscopic temperatures of the excited species formed at the final stage of acoustic collapse.

Figure 4 and data in Supporting Information show that an increase in *t*-BuOH concentration leads in most cases to a decrease in $\Delta T = T_v - T_r$. These two temperatures even become equal at 204 kHz. In other words, C_2* radicals are approaching thermal equilibrium while the bubble interior gets saturated with *t*-BuOH vapor. Equilibration of the rotational temperature is very fast, so that T_r is usually assumed to be close to the gas temperature. On the contrary, equilibration of T_v needs more collisions and therefore more time. As *t*-BuOH concentration increases, the number of hydrocarbon fragments in the bubbles increases and so does the frequency of collisions, hence lowering the vibrational temperature.

The most significant deviation from equilibrium (i.e., the highest ΔT) is observed in the presence of xenon, which may be related to the very high vibrational temperature reached. In general, in nonequilibrium plasmas the vibrational temperature is correlated with the electron temperature (T_e), $T_e > T_v$, or the electron density.[17] Xenon would provide a higher ionization degree than argon due to its lower ionization potential (12.13 eV for Xe; 15.76 eV for Ar).[18] It is noteworthy that xenon also enables strong vibrational excitation of $OH^\bullet$ radicals during the sonolysis of water at 20 kHz ultrasound (Table 2).

3.3. Kinetics of *t*-BuOH Sonolysis. Comparison of Figure 2 and Figure 4 demonstrates that in the first concentration domain (e.g., up to 2×10^{-3} M at 204 kHz) C_2* emission intensity increases in parallel to a decrease in T_v. Then, after reaching a maximum, C_2* emission intensity progressively decreases with a further increase in *t*-BuOH concentration. However, this decrease is not accompanied by any change in T_v: though C_2* emission is very low, relative intensities of $\Delta\nu$ = +1 and $\Delta\nu$ = 0 branches clearly correspond to the same values of T_v as at the maximum of C_2 emission.

In order to investigate the intrabubble conditions even at *t*-BuOH concentrations above SL quenching the formation of gaseous sonolytical products was followed at low (20 kHz) and high (362 kHz) US frequency, each time for two *t*-BuOH concentrations: at C_2 maximum emission (lower concentration) and at a concentration where SL continuum and C_2 emission are totally quenched (higher concentration). A significant sonochemical activity is observed in all four cases (Figure 5). According to the data on high temperature

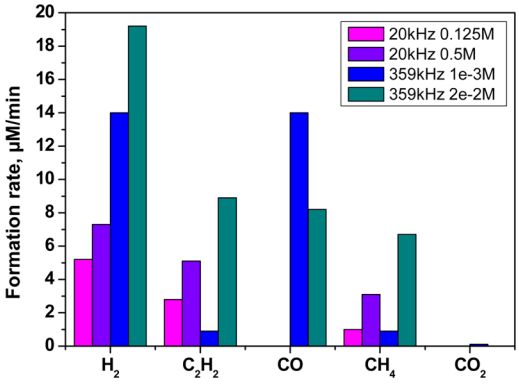

Figure 5. Formation rates of gaseous products as a function of ultrasonic frequency and *t*-BuOH concentration.

decomposition of hydrocarbons[19] the higher yield of C_2H_2 compared to CH_4 in the whole range of studied *t*-BuOH concentrations indicates that the intrabubble temperature reaches at least 1700K. Taking into account that C_2* radicals are formed from C_2H_2 via the intermediacy of $C_2H^\bullet$ or $CH^\bullet$ species[9] the extremely low light emission from C_2* at high concentration of *t*-BuOH can be attributed to the effective scavenging of $C_2H^\bullet$ and $CH^\bullet$ with primary products of *t*-BuOH sonolysis, such as $^\bullet CH_2C(CH_3)_2OH$ and $CH_3^\bullet$,[18] rather than to a sharp drop of temperature. Comparison of MBSL and sonochemical data allows to conclude that the formation of a nonequilibrium plasma inside the bubble is not necessarily accompanied by sonoluminescence. At high concentration of quenchers the de-excitation of light emitting species can occur via collisional nonradiative mechanisms without any significant impact on sonochemical activity.

While at high-frequency ultrasound CO is easily detectable in the outlet gases, at 20 kHz it is below the detection limit in the whole studied range of *t*-BuOH concentrations (Figure 5). Tauber et al.[20] concluded that in the absence of oxygen CO is formed during *t*-BuOH sonolysis through the oxidation of methyl radicals by $OH^\bullet$ radicals. Therefore, the lack of CO at low-frequency ultrasound may be explained by much lower yield of $OH^\bullet$ radicals at 20 kHz compared to high-frequency ultrasound as recently reported.[21]

It is interesting that we hardly observed any CO_2 emission whatever the studied experimental conditions (Figure 5). On the other hand, Tauber et al.[20] reported a CO_2 yield higher than that of CH_4 at similar conditions. This discrepancy is thought to be due to two principal reasons: (i) the mechanism of CO_2 formation which according to published data[20] involves CO oxidation by $OH^\bullet$ radicals or by water−gas shift reaction and (ii) the difference in reactor's configuration. Our experiments have been performed under continuous argon

DOI: 10.1021/jp509898p
J. Phys. Chem. B 2015, 119, 284−290

flow providing rapid removal of CO from the sonicated solutions. By contrast, the experiments of Tauber et al.[20] were done in a tightly closed vessel purged with argon prior sonication. Consequently, the formed CO remained in contact with the sonicated solution enabling its further oxidation.

4. CONCLUSIONS

In summary, the spectroscopic study of MBSL in aqueous *tert*-butyl alcohol solutions demonstrated that both the intensity and the shape of C_2* radical emission spectra are strongly influenced by the experimental parameters, such as *t*-BuOH concentration, ultrasonic frequency, and saturating gas. Addition of *t*-BuOH causes simultaneous quenching of water sonoluminescence and appearance of Swan band emission of C_2* intermediate. The optimal *t*-BuOH concentration for C_2* emission at 20 kHz is 100 times higher than at high-frequency ultrasound. Such striking difference can be explained by two reasons. First, smaller bubbles are formed under high-frequency ultrasound and the larger surface/volume ratio of small bubbles provides more efficient saturation of the bubble interior with *t*-BuOH vapors. Second, dynamics of bubbles are different, with high-frequency bubbles undergoing more oscillations before collapsing. This higher number of oscillations allows more *t*-BuOH evaporation into the bubbles; besides, hydrocarbon decomposition products accumulate at each oscillation and concentrate in the bubble. Hence a higher SL quenching is obtained for the same concentration of the solution.

The rovibronic temperatures of C_2* radicals obtained in this work using Specair software clearly pointed out the absence of thermal equilibrium inside the collapsing bubble ($T_v > T_r$). The increase in *t*-BuOH concentration leads to a decrease in ΔT indicating that C_2* radicals approach thermal equilibrium as the bubble interior gets saturated with *t*-BuOH vapor. The replacement of argon by xenon causes a significant increase of C_2* vibrational temperature most probably due to the lower ionization potential of Xe leading to higher electron temperature of the intrabubble nonequilibrium plasma. It is interesting to note that the MBSL of C_2* species studied in this work strongly correlates with the recently reported results on $OH^{\bullet}$ radicals MBSL which revealed nonequilibrium plasma formation during multibubble cavitation in water.

Kinetics of *t*-BuOH sonolysis demonstrates significant sonochemical activity in the whole range of studied *t*-BuOH concentrations even when the sonoluminescence is completely quenched. Moreover, the high yield of acetylene at these concentrations unequivocally indicates that the drastic conditions inside the cavitation bubbles are not necessarily accompanied by sonoluminescence.

■ ASSOCIATED CONTENT

Supporting Information

MBSL spectra of C_2* with subtracted continuum emission, their fits using Specair software, and the evolution of T_v and T_r as a function of *t*-BuOH concentration. This material is available free of charge via the Internet at http://pubs.acs.org.

■ AUTHOR INFORMATION

Corresponding Author

*(S.I.N.) E-mail: serguei.nikitenko@cea.fr. Telephone: +33 466339251.

Notes

The authors declare no competing financial interest.

■ ACKNOWLEDGMENTS

This work was supported by the French ANR program (ANR 2010 BLAN 0810 NEQSON).

■ REFERENCES

(1) Suslick, K. S.; Flint, E. B. Sonoluminescence from non-Aqueous Liquids. *Nature* **1987**, *330*, 553−555.
(2) Flint, E. B.; Suslick, K. S. The Temperature of Cavitation. *Science* **1991**, *253*, 1397−1399.
(3) Didenko, Y. T.; McNamara, W. B., III; Suslick, K. S. Hot Spot Conditions during Cavitation in water. *J. Am. Chem. Soc.* **1999**, *121*, 5815−5818.
(4) Navarro, N. M.; Pflieger, R.; Nikitenko, S. I. Multibubble Sonoluminescence as a Tool to Study the Mechanism of Formic Acid Sonolysis. *Ultrason. Sonochem.* **2014**, *21*, 1026−1029.
(5) Tanabashi, A.; Hirao, T.; Amano, T.; Bernath, P. F. The Swan System of C_2: A Global Analysis of Fourier Transform Emission Spectra. *Astrophys. J., Suppl. Ser.* **2007**, *169*, 472−484.
(6) Pellerin, S.; Musiol, K.; Motret, O.; Pokrzywka, B.; Chapelle, J. Application of the (0,0) Swan Band Spectrum for Temperature Measurements. *J. Phys. D: Appl. Phys.* **1996**, *29*, 2850−2865.
(7) (a) Ndiaye, A. A.; Pflieger, R.; Siboulet, B.; Nikitenko, S. I. The Origin of Isotope Effects in Sonoluminescence Spectra of Heavy and Light Water. *Angew. Chem., Int. Ed.* **2013**, *52*, 2478−2481. (b) Ndiaye, A. A.; Pflieger, R.; Siboulet, B.; Molina, J.; Dufreche, J.-F.; Nikitenko, S. I. Nonequilibrium Vibrational Excitation of OH Radicals Generated during Multibubble Cavitation in Water. *J. Phys. Chem. A* **2012**, *116*, 4860−4867. (c) Pflieger, R.; Brau, H.-P.; Nikitenko, S. I. Sonoluminescence from $OH(C^2\sum^+)$ and $OH(A^2\sum^+)$ Radicals in Water: Evidence for Plasma Formation during Multibubble Cavitation. *Chem.—Eur. J.* **2010**, *16*, 11801−11803.
(8) (a) Ashokkumar, M.; Hall, R.; Mulvaney, P.; Griezer, F. Sonoluminescence from Aqueous Alcohol and Surfactant Solutions. *J. Phys. Chem. B* **1997**, *101*, 10845−10850. (b) Price, G. J.; Ashokkumar, M.; Grieser, F. Sonoluminescence Quenching of Organic Compounds in Aqueous Solution: Frequency Effects and Implications for Sonochemistry. *J. Am. Chem. Soc.* **2004**, *126*, 2755−2762.
(9) Kruse, T.; Roth, P. Kinetics of C_2 Reactions during High-Temperature Pyrolysis of Acetylene. *J. Phys. Chem. A* **1997**, *101*, 2138−2146.
(10) Yasui, K. Influence of Ultrasonic Frequency on Multibubble Sonoluminescence. *J. Acoust. Soc. Am.* **2002**, *112*, 1405−1423.
(11) Brotchie, A.; Grieser, F.; Ashokkumar, M. Effect of Power and Frequency on Bubble-Size Distributions in Acoustic Cavitation. *Phys. Rev. Lett.* **2009**, *102*, 084302.
(12) Pears, R. W. B.; Gaydon, A. G. *The Identification of Molecular Spectra*; Chapman and Hall: Cambridge, U.K., 1976.
(13) Gaydon, A. G. *The Spectroscopy of Flames*; John Wiley: New York, 1975.
(14) Laux, C. O.; Spence, T. G.; Kruger, C. H.; Zare, R. N. Optical Diagnostics of Atmospheric Pressure Air Plasmas. *Plasma Sources Sci. Technol.* **2003**, *12*, 125−138.
(15) Okitsu, K.; Suzuki, T.; Takenaka, N.; Bandow, H.; Nishimura, R.; Maeda, Y. Acoustic Multibubble Cavitation in Water: A New Aspect of the Effect of a Rare Gas Atmosphere on Bubble Temperature and Its Relevance to Sonochemistry. *J. Phys. Chem. B* **2006**, *110*, 20081−20084.
(16) Ciawi, E.; Rae, J.; Ashokkumar, M.; Grieser, F. Determination of Temperatures within Acoustically Generated Bubbles in Aqueous Solutions at Different Ultrasound Frequencies. *J. Phys. Chem. B* **2006**, *110*, 13656−13660.
(17) Fridman, A. *Plasma Chemistry* ; Cambridge University Press: Cambridge, U.K., 2008.
(18) Well, E.; De Witt, J. M.; Jones, R. R. Comparison of Intense-Field Ionization of Diatomic Molecules and Rare-Gas Atoms. *Phys. Rev. A* **2002**, *66*, 013409.
(19) Lifshitz, A.; Frenklach, M. Mechanism of the High Temperature Decomposition of Propane. *J. Phys. Chem.* **1975**, *79*, 686−692.

DOI: 10.1021/jp509898p
J. Phys. Chem. B 2015, 119, 284−290

(20) Tauber, A.; Mark, G.; Schuchmann, H.-P.; von Sonntag, C. Sonolysis of tert-Butyl Alcohol in Aqueous Solution, J. *Chem. Soc. Perkin Trans.* **1999**, *2*, 1129−1135.
(21) Navarro, N. M.; Chave, T.; Pochon, P.; Bisel, I.; Nikitenko, S. I. Effect of Ultrasonic Frequency on the Mechanism of Formic Acid Sonolysis. *J. Phys. Chem. B* **2011**, *115*, 2024−2029.

DOI: 10.1021/jp509898p
J. Phys. Chem. B 2015, 119, 284−290